2022

Optimum geological storage depths for structural H2 geo-storage

Stefan Iglauer
Edith Cowan University, s.iglauer@ecu.edu.au

10.1016/j.petrol.2021.109498
Iglauer, S. (2021). Optimum geological storage depths for structural H2 geo-storage. *Journal of Petroleum Science and Engineering*. 212,109498.
https://doi.org/10.1016/j.petrol.2021.109498

Journal of Petroleum Science and Engineering 212 (2022) 109498

Contents lists available at ScienceDirect

Journal of Petroleum Science and Engineering

journal homepage: www.elsevier.com/locate/petrol

Optimum geological storage depths for structural H_2 geo-storage

Stefan Iglauer

Edith Cowan University, School of Engineering, 270 Joondalup Drive, 6027, Joondalup, Australia

ARTICLE INFO

Keywords:
Hydrogen underground storage
UHS
H_2 geo-storage
Structural trapping
Storage capacity
H_2 mass
Wettability
Buoyancy
Optimal storage depth

ABSTRACT

H_2 geo-storage has been suggested as a key technology with which large quantities of H_2 can be stored and withdrawn again rapidly. One option which is currently explored is H_2 storage in sedimentary geologic formations which are geographically widespread and potentially provide large storage space. The mechanism which keeps the buoyant H_2 in the subsurface is structural trapping where a caprock prevents the H_2 from rising by capillary forces. It is therefore important to assess how much H_2 can be stored via structural trapping under given geo-thermal conditions. This structural trapping capacity is thus assessed here, and it is demonstrated that an optimum storage depth for H_2 exists at a depth of 1100 m, at which a maximum amount of H_2 can be stored. This work therefore aids in the industrial-scale implementation of a hydrogen economy.

1. Introduction

Hydrogen geo-storage (UHS) has been identified as a potential solution to store large quantities of hydrogen, which is currently the main barrier to implementing an industrial-scale hydrogen economy (Lord et al., 2014; Zhang et al., 2016; Flesch et al., 2018; Heinemann et al., 2018; Tarkowski and Czapowski, 2018; ShiJessen and Tsotsis, 2020; Pan et al., 2021a). In UHS, H_2 is injected into subsurface geologic formations, and it can be withdrawn again at any time. One target formation currently investigated are sedimentary reservoirs, which are abundant and can have large storage capacities – such sedimentary reservoirs are also considered for CO_2 geo-sequestration (CGS, e.g. see IPCC 2005; Lackner, 2003), and they can classically also hold natural gas reserves, which are exploited industrially for a long time now (e.g. Dake, 1978). The buoyant gases (H_2, CH_4, CO_2) are stored by an impermeable seal layer, termed caprock by geologists (e.g. Dake, 1978; IPCC 2005; Wollenweber et al., 2010; Busch et al., 2008). Technically a caprock is also a sedimentary rock and it is also porous, but it has a very low permeability (e.g. Nelson, 2009; Sondergeld et al. 2010). The reason why the buoyant gases cannot percolate into the caprock is the high capillary entry pressure ($P_{c,e}$) of the caprock, which is again related to the very small pores in the caprock (Nelson, 2009).

However, if the buoyancy pressure exceeds $P_{c,e}$, then the buoyancy forces overcome the counter-acting capillary forces, and gas will indeed migrate upwards through the caprock (e.g. Iglauer et al., 2015a,b). This can be quantified by equation (1) – a buoyancy force – capillary force balance:

$$h = \frac{2\gamma cos\theta}{rg\Delta\rho} \quad \text{(equation 1)}$$

where h is the column height of gas which can be permanently immobilized beneath the caprock, g is the gravitational constant, $\Delta\rho$ is the difference between water density (ρ_w) and gas density (ρ_g), γ is the gas-water interfacial tension and θ is the water-rock-gas contact angle (e.g. Arif et al., 2016). Now it has been previously demonstrated that in the context of CGS, h varies with storage depth as $\Delta\rho$, γ and θ all vary significantly with depth (Iglauer, 2018). Consequently, a lower depth barrier exists below which CO_2 cannot be permanently stored by structural trapping (although note that interestingly below 15,000 m CO_2 is heavier than formation brine, and sinks spontaneously (due to gravitational forces) deep into the reservoir (Span and Wagner, 1996; Iglauer, 2018)). An optimum CO_2 storage depth also exists where a maximum amount of CO_2 can be stored. It is now hypothesized here that UHS also has an optimum storage depth (in terms of storing the largest mass of H_2), albeit H_2 will always be buoyant due to its high volatility in a geologic reservoir; Leachman et al. (2009). This hypothesis is examined in detail in the below section, and indeed the conclusion is reached that an optimum (technical) UHS depth exists, where a maximum amount of H_2 can be stored.

2. Methodology

It is clear that three parameters in equation (1) are affected by pressure and temperature, and thus depth, namely γ, $\Delta\rho$, and θ. To

E-mail address: s.iglauer@ecu.edu.au.

https://doi.org/10.1016/j.petrol.2021.109498
Received 25 May 2021; Received in revised form 6 September 2021; Accepted 14 September 2021
Available online 20 September 2021

conduct the analysis, a hydrostatic gradient of 10 MPa/km and a geothermal gradient of 30 K/km are assumed – which reflect common subsurface conditions (Dake, 1978; Meckel, 2010). Each parameter is therefore discussed in detail below.

2.1. The H_2-water density difference $\Delta\rho$

H_2 is an extremely highly compressible gas, a consequence is that the temperature and pressure ranges relevant in UHS (300–360 K and 0.1–20 MPa) only have a relatively insignificant effect on H_2 density (ρ_{H2}), Fig. 1. Compare this with CO_2, which undergoes a drastic change in density with increasing pressure and thus depth (Iglauer, 2018) – also ρ_{H2} is generally very low (e.g. ρ_{H2} is 3.5747 kg/m^3, while ρ_{CO2} is 100.22 kg/m^3 and ρ_{CH4} 30.897 kg/m^3 at 5 MPa and 330 K; Span and Wagner, 1996; Leachman et al., 2009). Furthermore, brine density (ρ_{brine}; note that formation water is typically saline, e.g. Mc Cain, 1990) slightly decreases with depth, Fig. 1 (assuming a constant salinity versus depth; Reveillere, 2013). Consequently, $\Delta\rho$ (= ρ_{brine} - ρ_{H2}) is only slightly affected by depth and only slightly decreases with depth.

2.2. The H_2-water interfacial tension γ

The H_2-water interfacial tension γ as a function of depth has not been evaluated previously. However, it has been demonstrated by laboratory experiments, that γ decreases very slightly with increasing pressure, but decreases strongly with increasing temperature (Chow et al., 2018). The γ-versus-depth profile has thus been inferred from these datasets (Chow et al., 2018), Fig. 1. Effectively, γ decreases linearly with depth, Fig. 1. For example, at a depth of 500 m, γ is 69.5 mN/m, and γ decreases slightly to 68.3 mN/m at 1000 m depth. However, γ always clearly remains relatively high and positive, and H_2 and brine are thus always immiscible at reservoir conditions (except the small amount of H_2 which chemically dissolves in the brine and the small amount of water which evaporates into the H_2 gas).

2.3. The H_2-water-rock contact angle θ

Importantly, θ increases relatively strongly with depth (mostly due to the increasing pressure, compare Iglauer et al. (2021) – note that here a rock surface which was exposed to 10^{-2} M stearic acid is assumed – such organic content is most realistic in the subsurface due to the prevailing reducing atmosphere, e.g. Stalker et al., 2013; Ali et al., 2019).

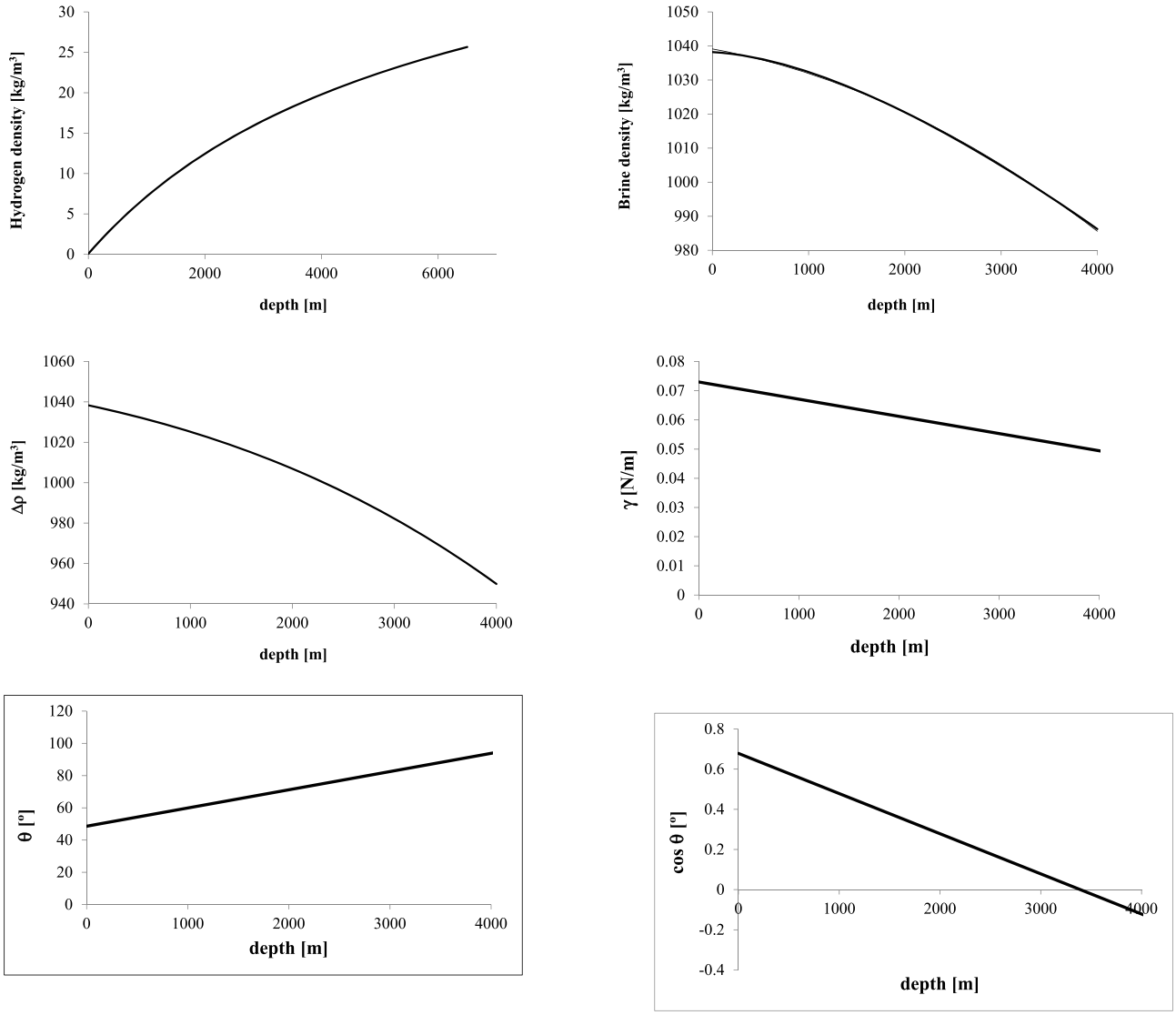

Fig. 1. Parameters required for structural trapping capacity assessment; (a) H_2 density, (b) brine density, (c) H_2-brine density difference $\Delta\rho$, (d) H_2-brine interfacial tension γ, (e) H_2-brine-caprock contact angle θ, (f) cos(θ) – all parameters are plotted against depth to illustrate the inherent dependencies.

Essentially a linear increase in θ with depth is predicted, compare Fig. 1 and Table 1 – precisely, θ increases from 44° at 0 m depth (= the surface) to 92° at 4000 m depth. This is a drastic increase, which sets a limit on H_2 storage capacities, see discussion below. This increase is caused by the increased H_2 density, which results in stronger H_2-rock intermolecular interactions, which again increase the affinity of the rock towards the H_2, e.g. Al-Yaseri et al. (2016, 2021). θ = 90° (neutral-wettability) is passed at 3700 m depth. Note that θ_{H2} is generally significantly smaller than the equivalent contact angle for CO_2 (θ_{CO2}), due to the lower H_2 density and the resulting lower H_2-rock intermolecular interactions (Iglauer, 2017; Iglauer et al., 2021; Ali et al., 2021; Pan et al., 2021b). Consequently, cosθ decreases linearly with storage depth, and importantly, cosθ intersects the x-axis also at 3700 m, Fig. 1.

2.4. H_2 column height h

H_2 column height *h* decreases monotonically with increasing depth, Fig. 2 (assuming a typical pore radius r of 50 nm, Nelson (2009); and g is 9.81 m/s^2). For instance, at 300 m storage depth, the H_2 column height is 183 m, which is reduced to 171 m at 500 m depth and 140 m at 1000 m depth. Importantly, h reaches a zero value at 3700 m depth, and storage below this threshold depth would result in H_2 percolating through the caprock as H_2 turned into the wetting phase at this point (θ > 90°; cosθ <0; see θ and cosθ discussion above).

Compare this with equivalent storage heights of CO_2 (in the context of CO_2 geo-sequestration); h_{CO2} is significantly lower (due to the higher wettability of CO_2 towards the rock surface; compare also Iglauer et al., 2021) and consequently the threshold depth for CO_2 is much more shallow (2400 m); Iglauer (2018).

2.5. The mass of H_2 which can be stored by structural trapping

Importantly, and indeed analogue to CO_2 storage, more relevant than h is the actual mass of H_2 (m_{H2}) which can be stored (Firoozabadi and Cheng, 2010). m_{H2} can be predicted via equation (2),

$$m_{H2} = \rho_{H2} h A \quad (2)$$

A is the averaged lateral area swept by H_2, and ϕ is the porosity of the storage rock (not the caprock) – here ϕ = 0.2 is assumed (which is a typical value for sandstone). A cannot be predicted easily as it also depends on reservoir geology, and a full-scale reservoir simulation is required to determine this parameter (e.g. see Lubon and Tarkowski, 2020; Al-Khdheeawi et al., 2017). A is assumed here to be A = 100 m × 100 m = 10^4 m^2 – although this may vary drastically based on the geology of the specific reservoir. Using these parameters and the parameters discussed above, the m_{H2} versus depth profile can be predicted, Fig. 2.

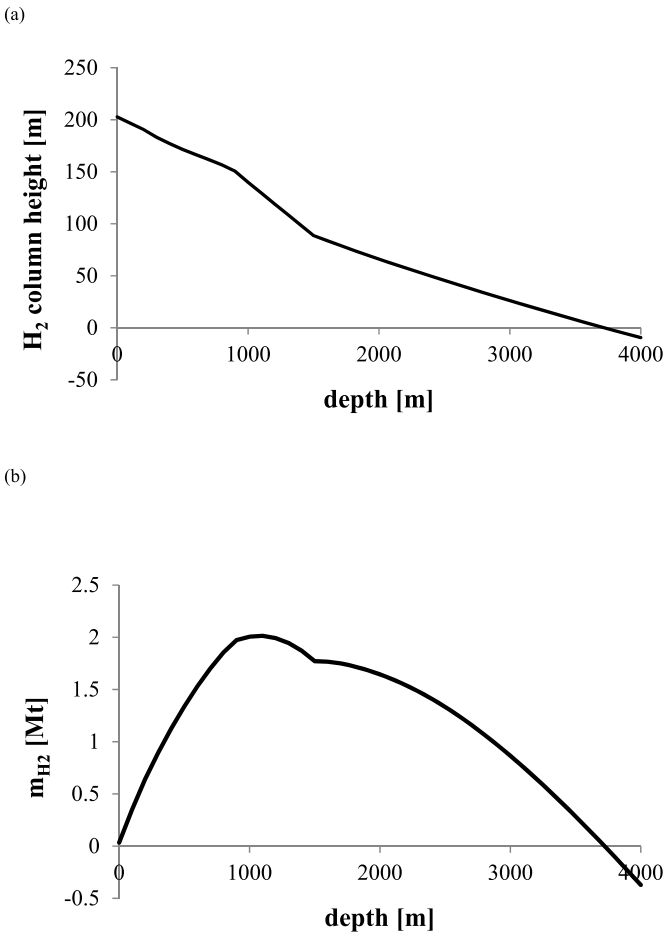

Fig. 2. H_2 structural storage capacity assessment, (a) H_2 column height *h* which can be permanently immobilized beneath the caprock, (b) mass of H_2 (m_{H2}) which can be stored by structural trapping.

Table 1
Best fit equations for the various petro-physical and physico-chemical parameters discussed here, as a function of reservoir depth (depth unit is meter here).

Parameter	Equation	R^2
ρ_{H2}	$\rho_{H2} = 0.8728 + 0.0065$ x depth $- 4 \times 10^{-7}$ x (depth)^2	0.9986
ρ_{brine}	$\rho_{brine} = 1039.1 - 0.0052$ x depth $- 2 \times 10^{-6}$ x (depth)^2	0.9996
Δρ	Δρ = 1038.3–0.0109 x depth $- 2 \times 10^{-6}$ x (depth)^2–2×10^{-10} x (depth)^3	1
γ	γ = 0.073–5.89286 × 10^{-6} x depth	0.9977
θ	θ = 48.603 + 0.0113 x depth	0.9763
Cosθ	cosθ = 0.6784–0.0002 x depth	0.9858
h	if d ∈[0; 900], then h = 201.68–0.0576 x depth if d ∈]900; 1500], then h = 242.47–0.1026 x depth if d ∈]1500; 4000], then h = 143.45–0.0387 x depth	for d ∈[0; 900]: R^2 = 0.9962 for d ∈[900; 1500]: R^2 = 1 for d ∈[1500; 4000]: R^2 = 0.9984
m_{H2}	if d ∈[0; 1000], then $m_{H2} = 0.0438 + 0.0031$ x depth $- 8 \times 10^{-7}$ (depth)^2–3×10^{-10} x (depth)^3 if d ∈]1000; 1500], then m_{H2} = 2.707–0.0006 x depth if d ∈]1500; 2200], then m_{H2} = 2.3938–0.0004 x depth if d ∈]2200; 2700], then m_{H2} = 3.3061–0.0008 x depth if d ∈]2700; 4000], then m_{H2} = 4.4827–0.0012 x depth	for d ∈[0; 1000]: R^2 = 0.9996 for d ∈]1000; 1500]: R^2 = 0.9394 for d ∈]1500; 2200]: R^2 = 0.9718 for d ∈]2200; 2700]: R^2 = 0.9978 for d ∈]2700; 4000]: R^2 = 0.9979

m_{H2} initially rapidly increases with depth, and reaches a maximum at 1100 m depth, Fig. 2. At higher depth m_{H2} decreases again, and reaches a zero value at 3700 m (as the H_2 column height is zero at this depth, see discussion above). At 300 m storage depth m_{H2} is 0.895 Mt, which increases to 1.33 Mt at 500 m and eventually 2.01 Mt at 1100 m.

This profile is somewhat similar to the m_{CO2} versus depth profile (for CGS, Iglauer, 2018), which also goes through a maximum, but at a slightly higher depth (1300 m). However, in absolute terms, m_{CO2} is generally much higher than m_{H2} (m_{CO2} is in the order of 100 Mt; while m_{H2} is only in the order of 1 Mt). Therefore, much less H_2 can be stored via this route when compared with CO_2. However, a storage capacity of 1 Mt H_2 is a high number generally, when compared to other current storage options (Zhang et al., 2016).

2.6. Correlations

Empirical correlations were calculated for each parameter (θ, γ, ρ, h, m_{H2}), these are listed in Table 1. Using these correlations initial UHS storage capacities can be predicted.

3. Conclusions and implications

H_2 geo-storage is currently explored as a feasible and economic solution to enable large-scale, widespread storage of large quantities of H_2. The main proposed storage mechanism for the buoyant H_2 in the subsurface is structural trapping, where a caprock provides a geologic seal through which H_2 cannot flow due to the high capillary entry pressure (of H_2) into the caprock. However, it is clear that H_2 can migrate upwards if buoyancy forces exceed the capillary forces – which again depend on the quantity (precisely the vertical H_2 column height h) of H_2 stored. This aspect is analysed here in more detail, and it is demonstrated that h is not a constant but declines monotonically with depth and reaches a zero value at 3700 m depth. Long term H_2 storage below this threshold depth is thus not advised as H_2 would percolate upwards through the caprock layer, due to wettability reversal at this depth. Importantly, the mass of H_2 which can be stored (m_{H2}) – which is the ultimate property of interest – goes through a maximum at 1100 m depth. There therefore exists a storage depth at which a maximum of H_2 can be stored. This work thus provides a fundamental assessment of H_2 structural storage efficiency, and aids in the implementation of a large-scale H_2 economy.

Declaration of competing interest

The author declares that he has no known competing financial interests or personal relationships that could have appeared to influence the work reported in this paper.

Nomenclature

p	pressure [Pa]
p_b	buoyancy pressure [Pa]
p_c	capillary pressure = pressure between wetting and non-wetting phase [Pa], i.e. pressure between H_2 and brine phase
ρ	density [kg/m^3]
ρ_{water}	density of water [kg/m^3]
ρ_{H2}	H_2 density [kg/m^3]
$\Delta\rho$	density difference between water and H_2 [kg/m^3]
h	H_2 plume height permanently immobilized by structural trapping [m]
d	depth [m]
θ	water contact angle [°]
γ	interfacial tension [N/m]
r	pore radius [m]
T	temperature [°C]
g	gravitational constant [m/s^2]
ϕ	porosity [-]
H_2	dihydrogen
A	surface area of 3D H_2 plume projected onto earth's surface [m^2]
m_{CO2}	mass of H_2 stored by structural trapping [kg]
R^2	Pearson's coefficient

References

Ali, M., Al-Anssari, S., Arif, M., Barifcani, A., Sarmadivaelh, M., Stalker, L., Lebedev, M., Iglauer, S., 2019. Organic acid concentration thresholds for ageing of carbonate minerals: implications for CO_2 trapping/storage. J. Colloid Interface Sci. 534, 88–94.

Ali, M., Jha, N.H., Al-Yaseri, A., Zhang, Z., Iglauer, S., Sarmadivaleh, M., 2021. Hydrogen wettability of quartz substrates exposed to organic acids – implications for hydrogen trapping/storage in sandstone reservoirs. J. Petrol. Sci. Eng. 207, 109081.

Al-Khdheeawi, E.A., Vialle, S., Barifcani, A., Sarmadivaleh, M., Iglauer, S., 2017. Impact of reservoir wettability and heterogeneity on CO_2-plume migration and trapping capacity. Int. J. Greenh. Gas Control 58, 142–158.

Al-Yaseri, A., Roshan, H., Lebedev, M., Barifcani, A., Iglauer, S., 2016. Dependence of quartz wettabiliuty on fluid density. Geophyscial Reseach Letters 43, 3771–3776.

Al-Yaseri, A., Fauziah, A., Wolff-Boenisch, D., Iglauer, S., 2021. Hydrogen wettability of clays: implications for underground hydrogen storage. Int. J. Hydrogen Energy (in press).

Arif, M., Barifcani, A., Lebedev, M., Iglauer, S., 2016. Structural trapping capacity of oil-wet caprock as a function of pressure, temperature and salinity. International Journal of Greenhouse Gas Control 50, 112–120.

Busch, A., Alles, S., Gensterblum, Y., Prinz, D., Dewhurst, D.N., Raven, M.D., Stanjek, H., Krooss, B.M., 2008. Carbon dioxide storage potential of shales. International Journal of Greenhouse Gas Control 2, 297–308.

Chow, Y.T.F., Maitland, G.C., Trusler, J.P.M., 2018. Interfacial tensions of (H2O + H2) and (H2O + CO2 + H2) systems at temperatures of (298–448) K and pressures up to 45 MPa. Fluid Phase Equil. 475, 37–44.

Dake, L.P., 1978. Fundamentals of Reservoir Engineering. Elsevier, Amsterdam.

Firoozabadi, A., Cheng, P., 2010. Prospects for subsurface CO_2 sequestration. AIChE J. 56 (6), 1398–1405.

Flesch, S., Pudlo, D., Albrecht, D., Jacob, A., Enzmann, F., 2018. Hydrogen underground storage—petrographic and petrophysical variations in reservoir sandstones from laboratory experiments under simulated reservoir conditions. Int. J. Hydrogen Energy 43 (45), 20822–20835.

Heinemann, N., Booth, M.G., Haszeldine, R.S., Wilkinson, M., Scafidi, J., Edlmann, K., 2018. Hydrogen storage in porous geological formations–onshore play opportunities in the midland valley (Scotland, UK). Int. J. Hydrogen Energy 43 (45), 20861–20874.

Iglauer, S., Al-Yaseri, A.Z., Rezaee, R., Lebedev, M., 2015a. CO_2-wettability of caprocks: implications for structural storage capacity and containment security. Geophys. Res. Lett. 42, 9279–9284.

Iglauer, S., Pentland, C.H., Busch, A., 2015b. CO_2-wettability of seal and reservoir rocks and the implications for carbon geo-sequestration. Water Resour. Res. 51 (1), 729–774. https://doi.org/10.1002/wrcr.21095. WR015553.

Iglauer, S., 2017. CO_2-Water-Rock wettability: variability, influencing factors, and implications for CO_2 geostorage. Accounts Chem. Res. 50, 1134–1142.

Iglauer, S., 2018. Optimum storage depth for structural CO_2 trapping. International Journal of Greenhouse Gas Control 77, 82–87.

Iglauer, S., Ali, M., Keshavarz, A., 2021. Hydrogen wettability of sandstone reservoirs: implications for hydrogen geo-storage. Geophys. Res. Lett. 48, 3. https://doi.org/10.1029/2020GL090814.

Intergovernmental Panel on Climate Change (IPCC), 2005. IPCC Special Report on Carbon Dioxide Capture and Storage, Prepared by Working Group III of the Intergovernmental Panel on Climate Change. Cambridge University Press.

Lackner, K.S., 2003. Climate change. A guide to CO_2 sequestration. Science 300, 1677–1678. https://doi.org/10.1126/science.1079033.

Leachman, J.W., Jacobsen, R.T., Penoncello, S.G., Lemmon, E.W., 2009. Fundamental equations of state for parahydrogen, normal hydrogen and orthohydrogen. J. Phys. Chem. Ref. Data 38 (3), 721–748.

Lord, A.S., Kobos, P.H., Borns, D.J., 2014. Geologic storage of hydrogen: scaling up to meet city transportation demands. Int. J. Hydrogen Energy 39 (28), 15570–15582.

Lubon, K., Tarkowski, R., 2020. Numerical simulation of hydrogen injection and withdrawal to and from a deep aquifer in NW Poland. Int. J. Hydrogen Energy 45 (3), 2068–2083.

Mc Cain, W.D., 1990. Properties of Petroleum Fluids. PennWell Books, Tulsa.

Meckel, T.A., 2010. Capillary Seals for Trapping Carbon Dioxide (CO2) in Underground Reservoirs. in: Developments and Innovation in Carbon Dioxide (CO2) Caputre and Storage Technology: Carbon Dioxide (CO2) Storage and Utilization, vol. 2. Woodhead Publishing Series in Energy No. 16, 185=202, GCCC Digital Publication #10-20.

Nelson, P.H., 2009. Pore-throat sizes in sandstones, tight sandstones, and shales. AAPG (Am. Assoc. Pet. Geol.) Bull. 93 (3), 329–340.

Pan, B., Xie, X., Iglauer, S., 2021a. Underground hydrogen storage: influencing parameters and future outlook". Adv. Colloid Interface Sci. 294, 102473.

Pan, B., Xie, X., Iglauer, S., 2021b. Rock-fluid interfacial tension at subsurface conditions: implications for H_2, CO_2 and natural gas geo-storage". Int. J. Hydrogen Energy 46 (50), 25578–25585.

Reveillere, A., 2013. Semi-analytical solution for brine leakage through passive abandoned wells taking account of brine density differences, 100. Transport in Porous Media, pp. 337–361.

Shi, Z., Jessen, K., Tsotsis, T.T., 2020. Impacts of the subsurface storage of natural gas and hydrogen mixtures. Int. J. Hydrogen Energy 45 (15), 8757–8773.

Span, R., Wagner, W., 1996. A new equation of state for carbon dioxide covering the fluid region from the triple-point temperature to 1100 K at pressures up to 800 MPa. J. Phys. Chem. Ref. Data 25 (6), 1509–1596. https://doi.org/10.1063/1.555991.

Stalker, L., Varma, S., Van Gent, D., Haworth, J., Sharma, S., 2013. South West Hub: a carbon capture and storage project. Aust. J. Earth Sci. 60 (1), 45–58.

Tarkowski, R., Czapowski, G., 2018. Salt domes in Poland–potential sites for hydrogen storage in caverns. Int. J. Hydrogen Energy 43 (46), 21414–21427, 2018.

Wollenweber, J., Alles, S., Busch, A., Krooss, B.M., Stanjek, H., Littke, R., 2010. Experimental investigation of the CO_2 sealing efficiency of caprocks. International Journal of Greenhouse Gas Control 4, 231–241. https://doi.org/10.1016/j.ijggc.2010.01.003.

Zhang, F., Zhao, P., Niu, M., Maddy, J., 2016. The survey of key technologies in hydrogen energy storage. Int. J. Hydrogen Energy 41, 14535–14552.